Electronic Supplementary Information (ESI)

Controllable Reconstruction of Lignified Biomass with Molecular Scissors to form Carbon Framework for Highly Stable Li Metal Battery

*Qi Lu, Chenyu Yang, Yang Xu, Zhan Jiang, Da Ke, Runze Meng, Sijiang Hu, Yuanzhen Chen, Chaofeng Zhang, Jianping Yang and Tengfei Zhou**

Q. Lu, Dr. C. Yang, Y. Xu, Z. Jiang, D. Ke, R. Meng, Prof. C. Zhang, Prof. T. Zhou
Institutes of Physical Science and Information Technology, Key Laboratory of Structure and Functional Regulation of Hybrid Material (Ministry of Education), Anhui University, Hefei 230601, China
E-mail: tengfeiz@ahu.edu.cn
Prof. S. Hu
Guangxi Key Laboratory of Low Carbon Energy Material, Guangxi Normal University, Guilin, 541004, China
Prof. Y. Chen
The State Key Laboratory for Mechanical Behavior of Materials, School of Materials Science and Engineering, Xi'an Jiaotong University, Xi'an 710049, PR China
Prof. J. Yang
State Key Laboratory for Modification of Chemical Fibers and Polymer Materials, College of Materials Science and Engineering, Donghua University, Shanghai 201620, China.

Qi Lu, Chenyu Yang and Yang Xu contributes equally to this work.

Experimental Procedures：

Preparation of biomass carbon sheet: First, the Pines should be cut into small pieces with dimensions of 2 cm*2 cm*0.5 cm. Next, the wood pieces are placed in a deionized water beaker, ensuring that the water covers the surface of the wood blocks, and left to stand overnight. Subsequently, the deionized water and wood blocks were introduced into a high-pressure reactor for a reaction process conducted at a heating temperature of 300 °C for a duration of 3 hours. Following the completion of the reaction, the reactor was depressurized and the wood blocks were subjected to drying procedures. These dried wood blocks were then positioned within a tube furnace for the purpose of high-temperature carbonization. The heating of the tube furnace was executed in a two-stage manner: initially at 260 °C for a period of 2 hours, followed by an elevation to 1000 °C for an additional 3 hours, with both stages maintained at a heating rate of 5 °C/min. Finally, the carbonized wood blocks are removed from the quartz tube and ground into carbon sheets with dimensions of 1 cm*1 cm*0.5 mm using sandpaper. The carbon sheets are washed multiple times with anhydrous ethanol and acetone to remove surface impurities before drying to obtain WTP (Water-Treated-Pine) samples.

For comparison, BTP (Base-Treated-Pine) and ATP (Acid-Treated-Pine) samples were prepared by immersing wood blocks in 0.1 M NaOH and 0.1 M H_2SO_4 solutions, respectively, to facilitate hydrothermal reactions, while all other conditions were held constant. Additionally, UTP (Untreated-Pine) samples were obtained by directly carbonizing wood blocks at high temperature without prior hydrothermal treatment, under consistent conditions. Circular samples with a diameter of 12 mm were fabricated by compressing nickel foam, copper foam, carbon paper, and carbon cloth using a press at a pressure of 300 kg cm^{-2}.

Preparation of biological carbon-based lithium cathode: In an argon-filled glove box, a number of lithium flakes were first heated to a molten state using a hot stage. Second, the WTP samples were held with tweezers and placed in the molten lithium flakes until the WTP samples were completely infiltrated by the lithium flakes.[1] Other BTP-Li samples, ATP-Li samples and UTP-Li samples were prepared using the same method. The infusion experiments of nickel foam, copper foam, carbon paper, carbon cloth electrode sheet with molten lithium metal were also made by the above method and named as Ni-Li, Cu-Li, Cp-Li, Cc-Li, respectively.

Material Characterization: The morphology, microstructure and deposition behavior of lithium metal on the samples were investigated by field emission scanning electron microscopy (FESEM), and the crystal structure and degree of graphitisation of the samples were characterized by X-ray powder diffraction (XRD). Raman spectra (Raman) of the samples were obtained using a confocal Raman microscope under 532 nm laser excitation. Based on the Brunauer-Emmett-Teller (BET) and Barrett-Joyner-Halenda (BJH) methods, respectively, the samples were analyzed using a specific surface area and pore size analyzer at 77 K for N_2 adsorption/desorption isotherms were measured to test the specific surface area and pore size distribution of the samples. The surface elemental composition and valence states of the samples were determined by X-ray photoelectron spectroscopy (XPS).

Electrochemical Measurements: The cells in question were assembled within a glove box, and comprehensive performance evaluations were conducted on electrochemical workstations (CH760 and DH7000C) and the NEWARE system. The electrolyte employed was 1.0 M $LiPF_6$ in a ternary solvent mixture of EC: DMC: EMC at a weight ratio of 1:1:1, supplemented with 1.0% VC. The diaphragm utilized was a Celgard 2325. These components were integrated into a CR-2032 button cell, which also included positive/negative shells, electrolyte, diaphragm, tabs, and shims. The assembled cells were tested on the Battery Test System (NEWARE BTS 8.0x). Furthermore, Electrochemical Impedance Spectroscopy (EIS) measurements were conducted on a CH760 Electrochemical Workstation across a frequency range of 0.01-100 kHz, while Exchange Current Density testing was performed on a DH7000C Electrochemical Workstation. All cells were ultimately evaluated on the NEWARE BTS 8.0x Electrolyte/Separator System.

COSMOL Multiphysics: Lithium deposition and molten lithium infiltration simulations were performed using the COMSOL Multiphysics. The tertiary current distribution (PNP) model, horizontal set phase field and two-phase flow in porous media were used to study the current density distribution and the reaction rate of lithium evolution.[2]

Tertiary current distribution

Phase field

The phase field variable is used to set the electrolyte volume fraction in the electrolyte charge transport model, while the velocity field in the Phase Field interface is based on the reaction rate of

the lithium evolution reaction. When using the phase field method, both the electrode and the electrolyte are described on the same domain. The Phase Field interface is used to track the deformation of the cathode surface during deposition. For simplicity, the anode position remains fixed in the model.[3]

In the Phase Field interface, two-phase fluid dynamics is governed by the Cahn-Hilliard equation and tracks the diffusion of the separated immiscible phases Interface. The latter is defined as dimensionless phase field variables ϕ from -1 in the electrolyte domain to 1 in the deposition region In COMSOL Multiphysics, the Cahn-Hilliard equation is split into two equations：

$$\frac{\partial \phi}{\partial t} + u \cdot \nabla \phi = \nabla \frac{\gamma \lambda}{\varepsilon^2} \nabla \psi$$

$$\psi = -\nabla \cdot \varepsilon^2 \nabla \phi + (\phi^2 - 1)\phi$$

where u is the fluid velocity (m/s), γ is the mobility ($m^3 \cdot s/kg$), λ is the mixed energy density (N), and ε (m) is the interface thickness parameter. ψ variables are called phase field helpers. The following equation relates the mixed energy density and interfacial thickness with the surface tension coefficient:

$$\sigma = \frac{2\sqrt{2}\lambda}{3\ \varepsilon}$$

In this model, the interface thickness parameter is set to $\varepsilon = h_{max}/16$, where h_{max} is the largest mesh element size in the domain. The mobility parameter γ determine the time scale of Cahn-Hilliard diffusion and must be chosen carefully, usually large enough to keep the interface thickness constant, but small enough to not overattenuate the convective term. A suitable γ value is the maximum velocity magnitude that appears in the model. In the Phase Field interface, the volume fractions for each fluid are as follows

$$V_{f1} = \frac{1-\phi}{2},\ V_{f2} = \frac{1+\phi}{2}$$

The volume fraction v_{fl} changed from 1 in the electrolyte domain to 0 in the deposition region. The δ function of the phase field is approximated as:

$$\delta = \frac{3}{4}(1-\phi^2)|\nabla\phi|$$

The velocity field used in the phase field variable transport equation is calculated based on the lithium deposition reaction current density:

$$u = n \cdot \left(-\frac{i_{loc} M_{Li}}{2F\,\rho_{Li}}\right)$$

where i_{loc} is the local current density, M_{Li} is the molar mass, and ρ_{Li} is the density of lithium. The formula for calculating the interface normal n is as follows:

$$n = \frac{\nabla\phi}{|\nabla\phi|}$$

A phase field variable with a value of 1 enters the domain from the bottommost boundary of the domain, which is specified by the entrance boundary condition, and the rest of the boundary is specified using the exit boundary condition.

2PNP model

The flux of each ion in the electrolyte is given by the Nernst-Planck equation, where the effective diffusion coefficient and mobility are used

$$N_i = -D_{i,eff}\nabla c_i - z_i u_{i,eff} F c_i \nabla\phi_l$$

where N_i denotes the transfer vector (mol/(m^2 ·s)), c_i denotes the concentration in the electrolyte (mol/m^3), z_i denotes the charge of ionic species, $u_{i,\,eff}$ denotes the mobility of charged species m^2/s·J·mole)), and F denotes Faraday's constant (As/mole). ϕ_l represents the potential (V) in the electrolyte. The effective diffusion coefficient is defined by the electrolyte volume fraction

$$D_{i,eff} = \varepsilon_l D_i$$

where ε_l is the electrolyte volume fraction. ε_l is defined in terms of the phase field volume fraction v_{fl}, changing from 1 in the electrolyte domain to 0 in the deposition region. In addition, the mass balance equation is:

$$\frac{\partial \varepsilon_l c_i}{\partial t} + \nabla \cdot N_i = R_i$$

One equation for each substance, i = 1, 2. The rate of the electrochemical reaction is

$$R_i = -\frac{v_i i_v}{nF}$$

Electrolyte volume fraction compensation ensures that the electrodes do not act as reservoirs for lithium and sulfate ions. The electrically neutral condition is expressed by the following expression:

$$\sum_i z_i c_i = 0$$

Lithium plating kinetics

Increasing the kinetics of side reactions allows us to study the competing reactions on the electrode surface during charging.[4] Taking into account the equilibrium potential of the plating reaction (0 V vs. Li/Li$^+$), an electrode potential equal to or below zero indicates the start of lithium plating. Assuming that the plating reaction is completely irreversible, the Butler-vol mer kinetics is used to describe the rate of the plating reaction:

$$i_{loc} = i_0\left[exp\left(\frac{\alpha_a F\eta_{plating}}{RT}\right) - exp\left(\frac{-\alpha_c F\eta_{plating}}{RT}\right)\right]$$

where overvoltage is defined as: $\eta_{plating}=\varphi_s - \varphi_l E_{eq,plating}$

The Arrhenius equation is used to model temperature changes in properties such as exchange current density and diffusion coefficient. The material library uses the Arrhenius equation to provide a temperature-dependent electrolyte diffusion coefficient.

The main reactions of lithium interactions in porous matrices are as follows:

$$C_6 + Li^+ + e^- \rightarrow LiC_6$$

In lithium metal batteries, lithium metal is deposited on the negative electrode during charging, and lithium metal is deposited at the negative electrode as current flows through the battery. This is shown in the following formula

$$Li^+ + e^- \rightarrow Li(s)$$

The model consists of a negative electrode (graphite) and an intermediate separator to represent the conservation of charge in the battery cell, electrolyte and solid electrodes, and conservation of matter in the electrolyte and active material. The lithium deposition reaction current density on the

cathode surface is added to the domain as a source term, and the phase field δ function is used to specify the deposition reaction along the deformation boundary:

$$i_v = i_{loc}\delta$$

The boundary conditions for the anode surface are:

$$N_{Li+} \cdot n = -\frac{i_{loc}}{2F}$$

where n denotes the normal vector of the boundary. For simplicity, the anode surface in this model is not deformed. The other boundaries are insulated boundaries

$$N_{M^{X+}} \cdot n = 0$$

For sulfate ions, the insulation conditions apply to all boundaries:

$$N_{N^{Y-}} \cdot n = 0$$

The composition of the electrolyte is set according to the following formula

$$c_{Li+} = c_0$$

$$c_{N^{Y-}} = c_0$$

The above electrochemical model was established using the "tertiary current distribution, Nernst-Planck equation".

Multiphase flow in porous media

The Phase Transport in Porous Media interface follows an independent equation for the volume fraction s_i of wet or non-wet fluid i:

$$\frac{\partial}{\partial t}(E_p \rho_i s_i) + \nabla \cdot \left(-\rho_i \kappa \frac{\kappa_{ri}}{\mu_i}(\nabla p_i - \rho_i g) \right) = Q_i = 0$$

where ε_p is the porosity and permeability (m^2), κ_{ri} is the relative permeability (a function of the saturation of a given fluid), μ_i is the dynamic viscosity of the fluid (Pa·s), p_i is the pressure (Pa), and ρ_i is the fluid density of phase i(kg/m^3)。 Since the sum of the volume fractions of the two phases is 1, the rest of the volume fractions can be calculated according to the following formula

$$s_1 = 1 - s_2 \frac{1}{(s_w)^{1/\lambda_p}}$$

The calculation of the capillary pressure P_c varies with the wet phase saturation S_w (S_2 in this model) and the inlet capillary pressure P_{ec}. Using the Brooks-Corey model, the capillary pressure is calculated according to the equation:

$$p_c = p_{ec}$$

where λp is the pore distribution index. According to the Brooks-Corey model, the relative permeability of the wet and non-wet phases is given by

$$\kappa_{rs_w} = (s_w)^{\left(3 + 2/\lambda_p\right)}$$

$$\kappa_{rs_n} = s_n^2\left(1 - (1 - s_n)^{\left(1 + 2/\lambda_p\right)}\right)$$

The Law of Reach interface combines the law of reach with the continuity equation:

$$\frac{\partial}{\partial t}(\rho\varepsilon_p) + \nabla \cdot \rho\left[-\frac{\kappa}{\mu}(\nabla p)\right] = 0$$

where the density ρ and the dynamic viscosity μ are the average values of wet and non-wet fluids.

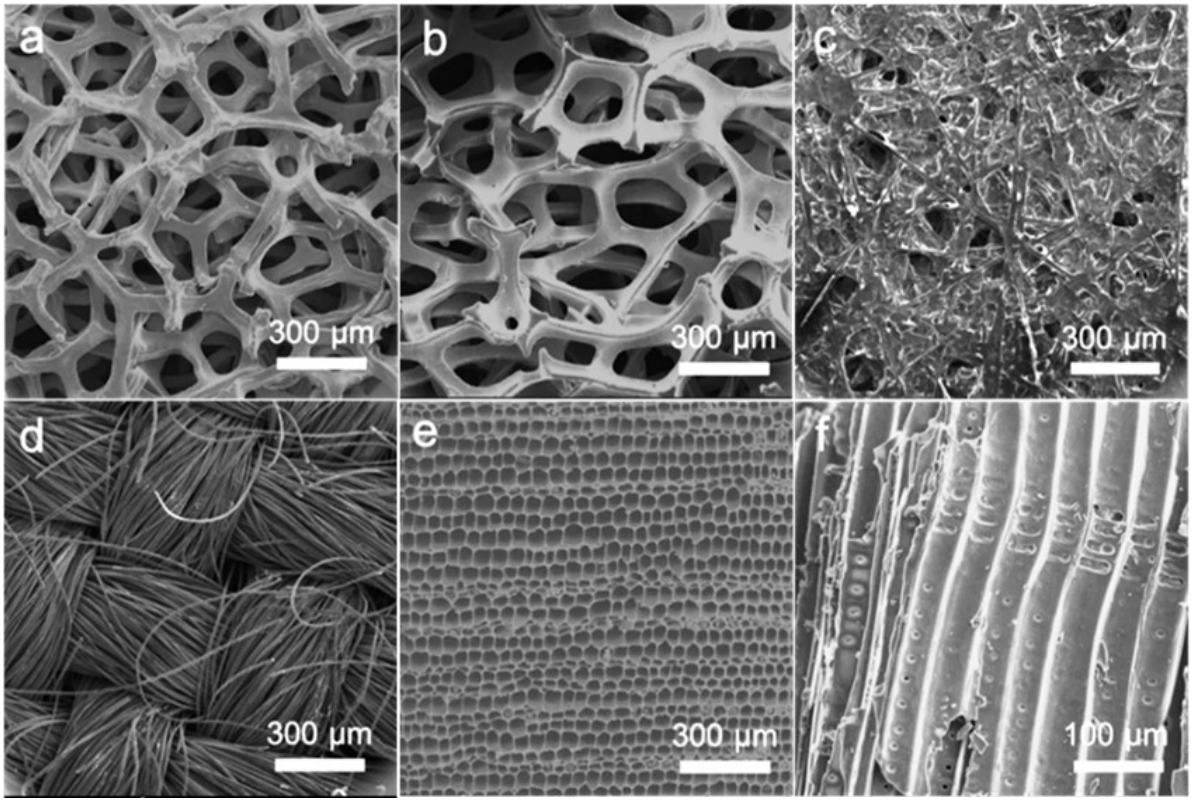

Figure S1. SEM images of (a) copper foam, (b) nickel foam, (c) carbon paper, (d) carbon cloth, (e) biomass carbon cross section and (f) biomass carbon longitudinal section.[2]

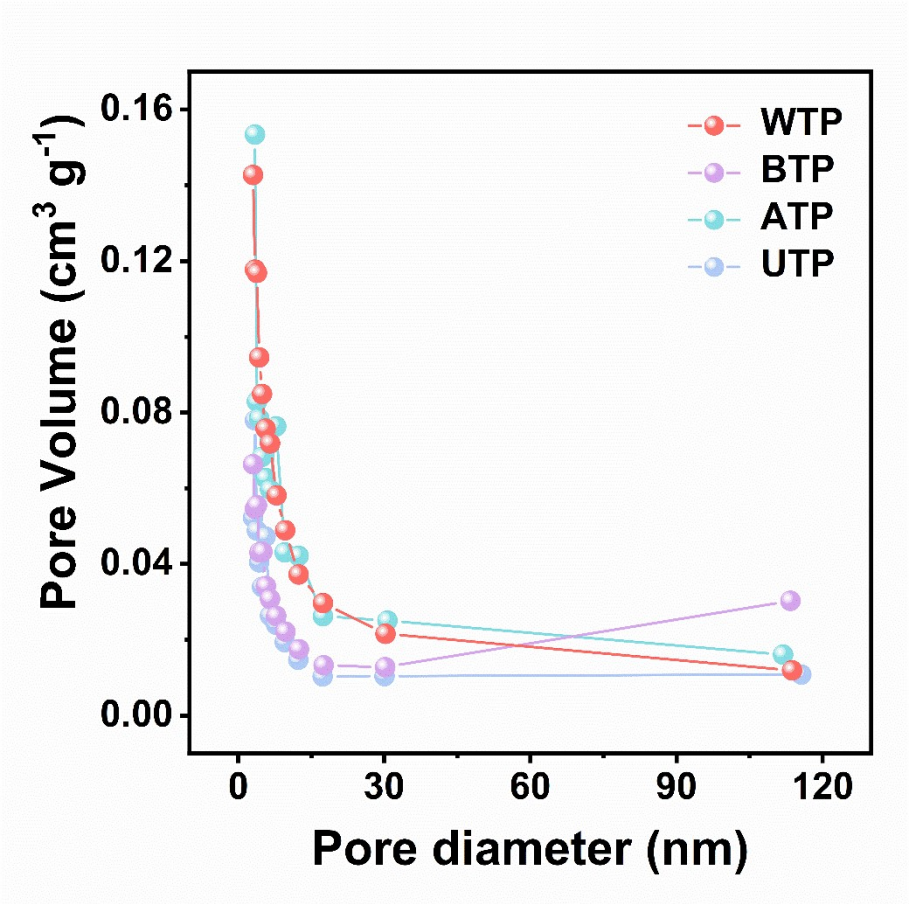

Figure S2. Pore size distribution diagram of WTP, BTP, ATP and UTP.

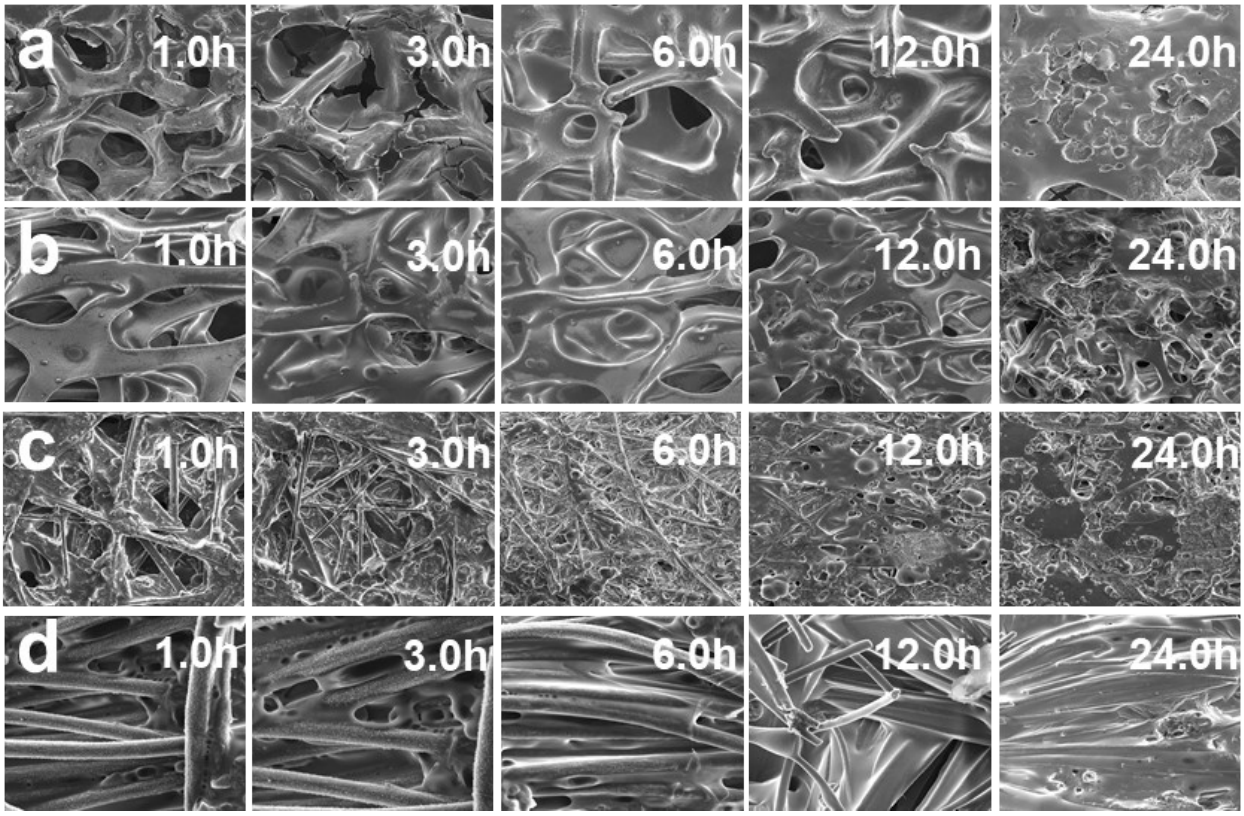

Figure S3. SEM images of lithium deposition behavior of (a) copper foam, (b) nickel foam, (c) carbon paper, (d) carbon cloth.

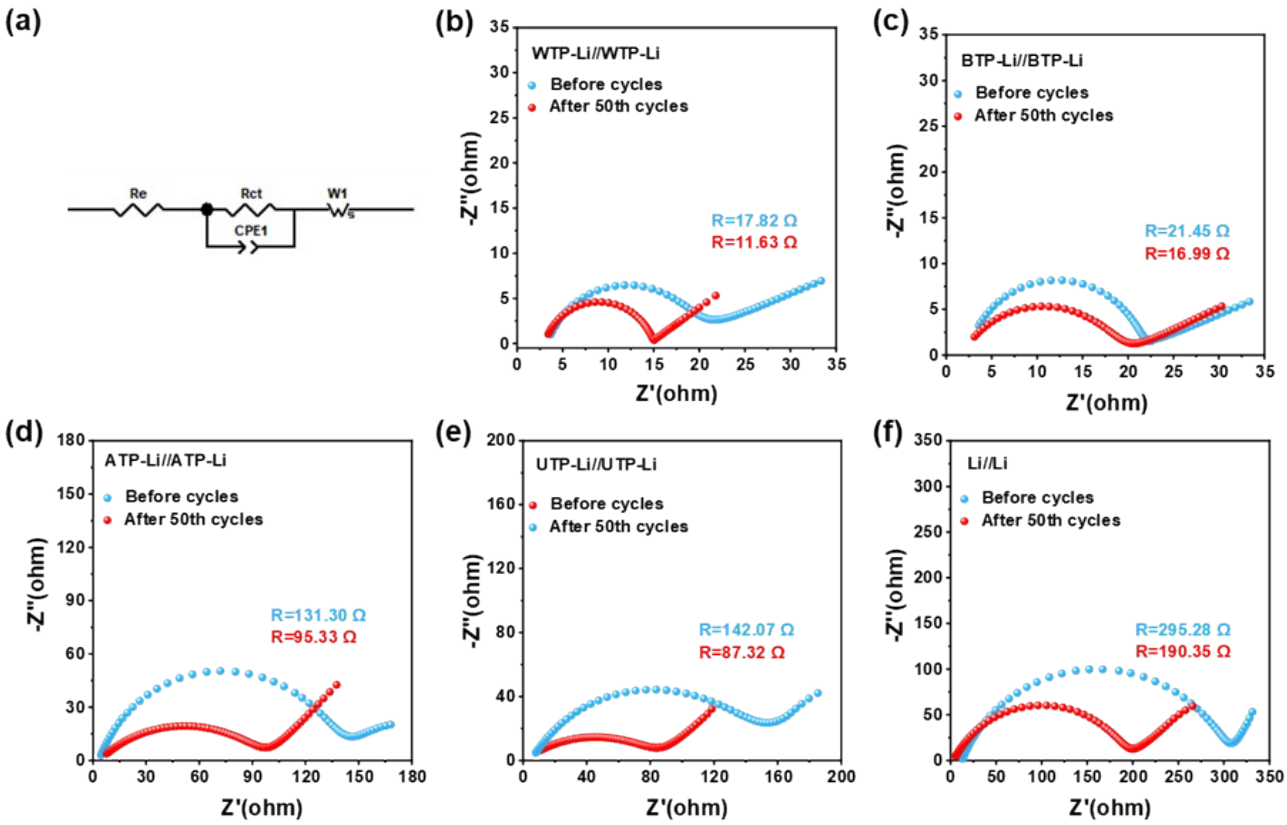

Figure S4. (a) electrochemical impedance equivalent circuit diagram, (b) WTP-Li electrode, (c) BTP-Li electrode, (d) ATP-Li electrode, (e) UTP-Li electrode, (f) bare Li electrode of EIS.

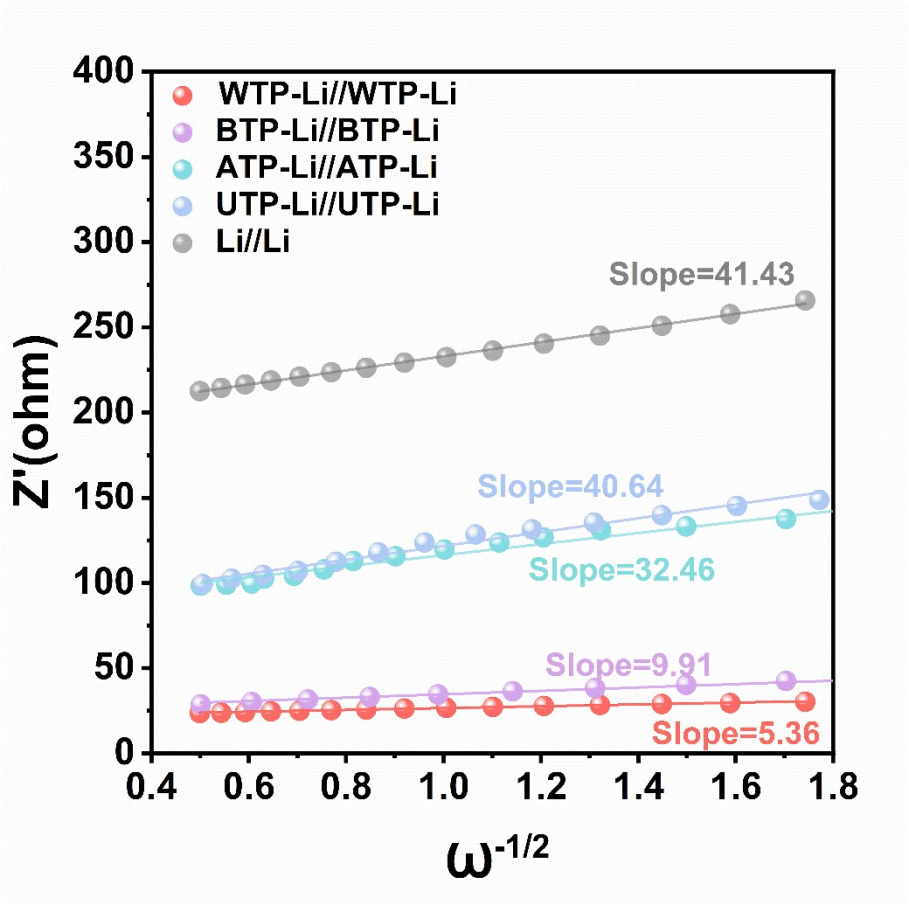

Figure S5. According to the Nestor diagram corresponding to the impedance real part and low frequency $\omega^{-1/2}$ diagram.

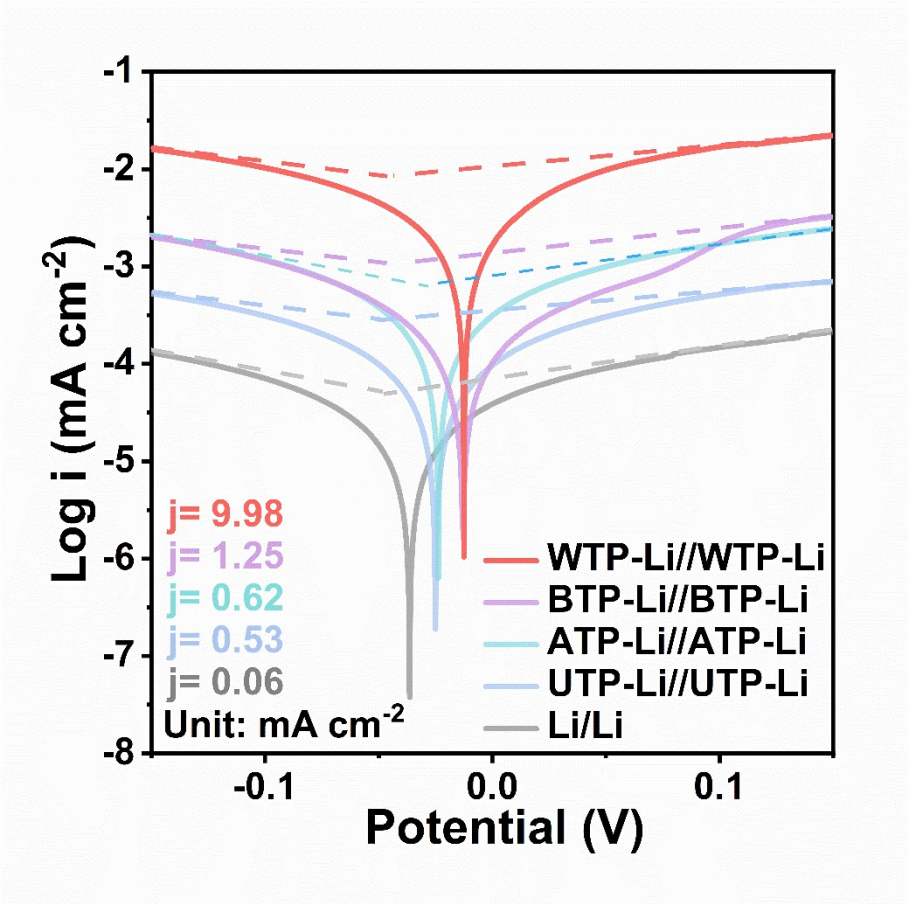

Figure S6. Tafel test graph.

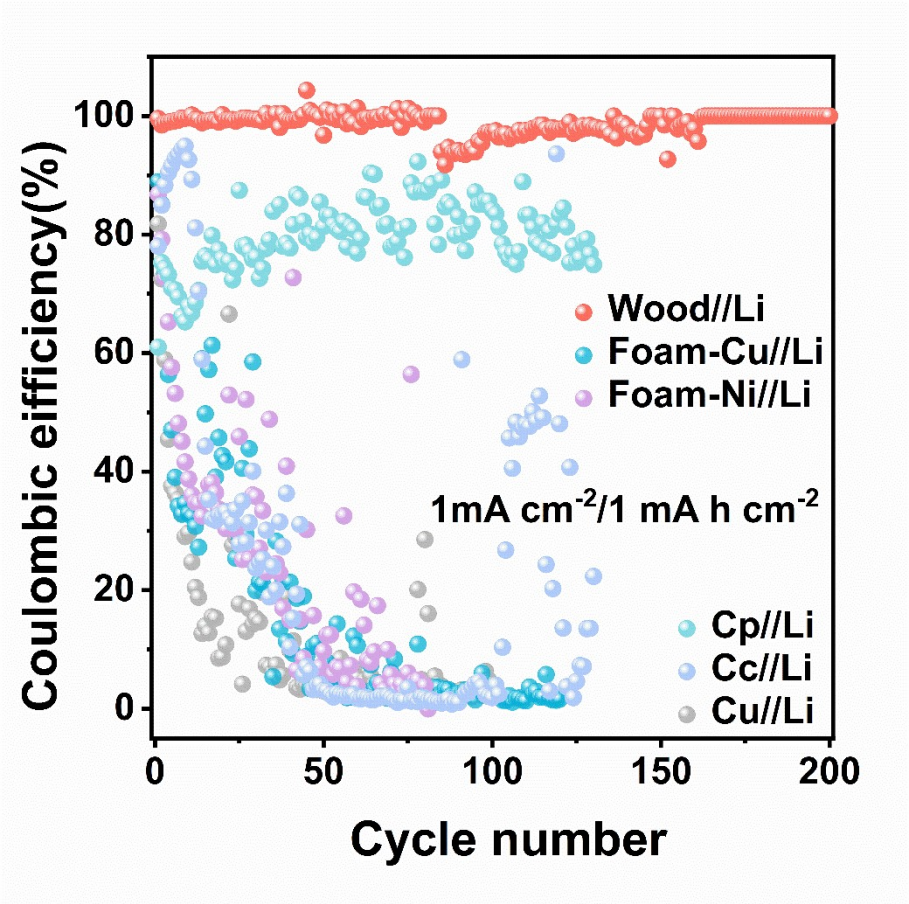

Figure S7. Electrochemical performance of a half cell assembled with different lithium three-dimensional composite electrodes.

Reference

1 Y. Qian, Z. Zhu, Y. Li, Z. Pan, L. Wang, J. Tian, H. Zhou, N. Lin and Y. Qian, *Energy Storage Mater.,* 2022, **47**, 620.

2 S. Ni, J. Sheng, C. Zhang, X. Wu, C. Yang, S. Pei, R. Gao, W. Liu, L. Qiu and G. Zhou, *Adv. Funct. Mater.,* 2022, **32**, 2200682.

3 Z. Yang, W. Liu, Q. Chen, X. Wang, W. Zhang, Q. Zhang, J. Zuo, Y. Yao, X. Gu, K. Si, K. Liu, J. Wang and Y. Gong, *Adv. Mater.,* 2023, **35***,* 2210130.

4 L. Lin, K. Yue, L. Xia, X. Yan, H. Zheng, Y. Zhang, B. Sa, J. Li, L. Wang, J. Lin, Y. Liu, G. Wei, D. Peng and Q. Xie, *Angew. Chem.,* 2024, **136**, e202319847.